Applied Surface Science 525 (2020) 145867

Contents lists available at ScienceDirect

Applied Surface Science

journal homepage: www.elsevier.com/locate/apsusc

Full Length Article

Detonation exfoliated mechanism of graphene-like MoS_2 prepared by the intercalation-detonation method and promising exfoliation for 2D materials

Fan Yang[a,b,1], Kuaishe Wang[a,b,*], Ping Hu[a,b,*,1], Xiaoyu Wang[a,b], Tian Chang[a,b], Zhenyu Chen[a,b], Jie Deng[a,b], Pengfa Feng[c], Alex A. Volinsky[d]

[a] School of Metallurgy Engineering, Xi'an University of Architecture and Technology, Xi'an 710055, People's Republic of China
[b] State Local Joint Engineering Research Center for Functional Materials Processing, Xi'an University of Architecture and Technology, Xi'an 710055, People's Republic of China
[c] Jinduicheng Molybdenum Co., Ltd., Xi'an 710077, People's Republic of China
[d] Department of Mechanical Engineering, University of South Florida, Tampa, FL 33620, USA

ARTICLE INFO

Keywords:
Graphene-like MoS_2
Intercalation-detonation method
Detonation exfoliated mechanism
Layered structure
2D materials

ABSTRACT

Due to its intrinsic band gap, graphene-like MoS_2 has been widely studied. It has a significant potential for applications in novel electronic, semiconductor and optoelectronic devices. For comparison, five kinds of explosion mass ratios were used to investigate the detonation exfoliated mechanism of graphene-like MoS_2 prepared by the intercalation-detonation method. Bulk WS_2 and h-BN powders were also exfoliated by detonation method. X-ray diffraction, X-ray photoelectron spectroscopy and high-resolution transmission electron microscopy results show that pure MoS_2 nanosheets with hexagonal crystal structure were obtained with the 1:1 detonation mass mixture ratio of picric acid and MoS_2 powder. 2:1 detonation mass mixture ratio produced monolayer MoS_2 nanosheets, but a spot of MoS_2 can also be decomposed to Mo_2S_3 and S at high explosion temperature. The higher the detonation mass mixture ratio, the more MoS_2 is proposed to be decomposed. The 1:1 detonation mass mixture ratio is the most suitable to exfoliate graphene-like MoS_2 nanosheets. Bulk WS_2 and h-BN were detonation exfoliated to single and few layers nanosheets successfully, showing the promising wide range of application of exfoliation in two-dimensional materials.

1. Introduction

As one of the most studied two-dimensional (2D) transition metal dichalcogenides (TMDs) materials, graphene-like MoS_2 shows significant potential for novel electronic, semiconductor and optoelectronic devices due to its intrinsic band gap [1–3]. Layered bulk MoS_2 has strong covalent Mo-S bonds in each layer with weak Van-der-Waals bonds between the layers, and each layer has a thickness of 6.5 Å [4–6]. Bulk MoS_2 is a semiconductor with an indirect bandgap of 1.2 eV, while monolayer MoS_2 is a 1.8 eV direct bandgap semiconductor, which is different from zero bandgap conductive graphene [7–11].

Due to layered structure and weak Van-der-Waals bonds between the layers, different kinds of "top-down" exfoliation approaches have been explored to prepare graphene-like MoS_2 nanosheets, including micromechanical exfoliation [12,13], sonication-assisted liquid-exfoliation [14–17], shear exfoliation [18–20] and chemical exfoliation [21–23]. Exfoliation of MoS_2 can start from abundant natural crystals or intentionally doped synthetic crystals by "top-down" methods [24]. However, production of monolayer MoS_2 nanosheets by mechanical exfoliation methods has been challenging so far because of the low yield of monolayer products, complicated procedures and lengthy reaction processes. In addition, some procedures may transform MoS_2 from its pristine hexagonal structure (2H phase) to trigonal 1 T phase, such as lithium intercalation reaction [21–23]. This change from trigonal prismatic to octahedral coordination of Mo compromises the semiconducting properties of the sheets [24].

It is well known that fast decomposition of explosives produces high temperature and powerful shock wave, which can induce exfoliation and synthesis of materials. This kind of detonation method has been used to prepare nanophase materials, such as diamond, graphene, metal oxide nanoparticles, metal nanoparticles and compounds [25–28]. A novel intercalation-detonation method to prepare graphene-like MoS_2 and the oxidation layering mechanism of intercalation has been reported in our previous study, which for the first time used oxygen-

* Corresponding authors at: School of Metallurgy Engineering, Xi'an University of Architecture and Technology, Xi'an 710055, People's Republic of China.
E-mail addresses: wangkuaishe888@126.com (K. Wang), Pinghu1985@126.com (P. Hu).
[1] These authors contributed equally.

https://doi.org/10.1016/j.apsusc.2020.145867
Received 1 January 2020; Received in revised form 14 February 2020; Accepted 22 February 2020
Available online 24 February 2020
0169-4332/

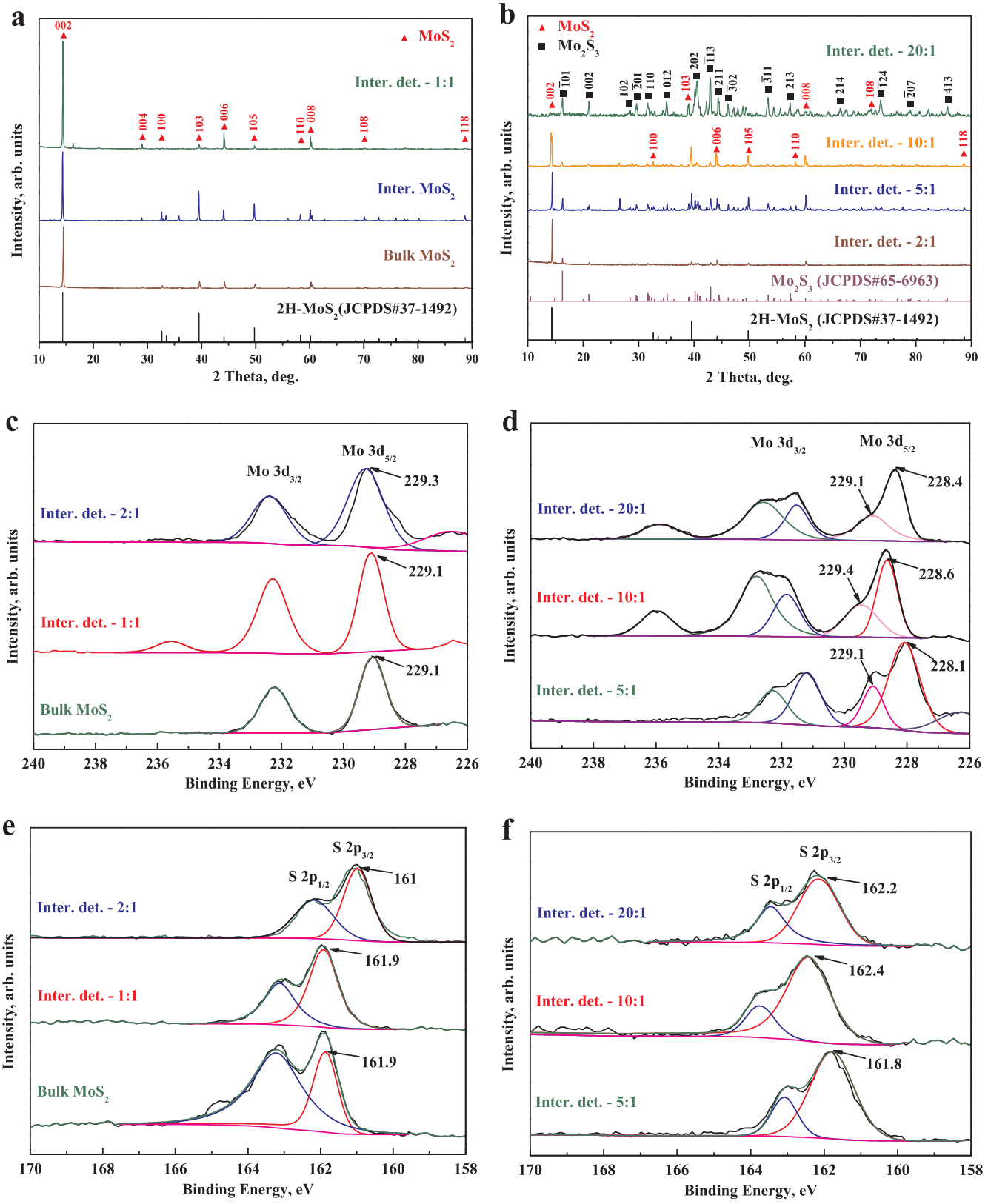

Fig. 1. XRD patterns and high-resolution XPS spectra of MoS_2 materials: (a) Bulk, intercalation and 1:1 mixture ratio intercalation-detonation MoS_2; (b) intercalation-detonation MoS_2 detonated with of 2:1, 5:1, 10:1 and 20:1 mixture ratio; (c, e) Mo 3d and S 2p spectra of bulk, 1:1 and 2:1 mixture ratio intercalation-detonation MoS_2; (d, f) Mo 3d and S 2p spectra of intercalation-detonation MoS_2 detonated under mixture ratio of 5:1, 10:1 and 20:1.

Table 1
Mass fraction of MoS_2 and Mo_2S_3 crystals with the Mo $3d_{1/2}$ peak locations and at% ratio of S/Mo from XPS.

Samples	*W* (MoS_2), wt%	*W* (Mo_2S_3), wt%	Mo $3d_{5/2}$, eV	S/Mo
Bulk	100	0	229.1	2
1:1	97.9	2.1	229.1	2
2:1	69.7	30.3	229.3	1.676
5:1	50.7	49.3	228.1/229.1	1.618
10:1	32.6	67.4	228.6/229.4	0.862
20:1	12.9	87.1	228.4/229.1	0.729

containing groups as intercalation compound of layered structure and took advantage of the explosion technology to exfoliate intercalated MoS_2 [29,30].

Herein, the detonation exfoliated mechanism of graphene-like MoS_2 was investigated by using different explosion ratio with X-ray diffraction, X-ray photoelectron spectroscopy, high resolution transmission electron microscopy and atomic force microscopy as characterization methods. Bulk WS_2 and h-BN powders were also exfoliated by detonation method to reflect the practicality of exfoliation in 2D materials.

2. Experimental methods

2.1. Oxidation intercalation of MoS_2

Preparation of intercalated MoS_2 is described in previous publication [30], and the intercalation details are as follows. A 2:1 mass ratio of commercial MoS_2 powder and $NaNO_3$ crystals were dissolved in a certain volume of 98% concentrated sulfuric acid, where the concentration of MoS_2 powder dispersed in sulfuric acid was 0.25 g/ml. The reaction flask was placed in ice bath with violent stirring, and a certain quantity of $KMnO_4$ (three times the mass of the MoS_2 powder) was added slowly to avoid sudden increase in temperature. After 120 min reaction, the flask was heated to 35 °C for 60 min and 90 °C held for 5 min in series. The reactive solution was diluted during stirring and a certain amount of warm deionized water was added slowly during 35 °C to 90 °C reaction. (5)% hydrogen peroxide solution was added into the solution after the heating process to remove $KMnO_4$. The solution was vacuum filtered and thoroughly washed with deionized water until the pH of the filtrate became neutral. After filtration, the intercalated MoS_2 was obtained.

2.2. Detonation exfoliation of MoS_2, WS_2 and h-BN

Exfoliation was performed next by placing premixed intercalation MoS_2 and picric acid in a sealed stainless steel pressure vessel. The 1:2, 1:1, 2:1, 5:1, 10:1 and 20:1 mixture mass ratios of picric acid and MoS_2 powder were selected to investigate the detonation exfoliate mechanism of graphene-like MoS_2. Detonation was induced by rapid heating at 50 °C/min to 400 °C. After that, the vessel was cooled in air, and generated gaseous products were released, while solid products were collected. The final samples of graphene-like MoS_2 nanosheets were obtained by washing and dispersing the collected solid products in deionized water and absolute ethanol. Bulk WS_2 and h-BN were also exfoliated by detonation process using 1:1 mixture mass ratio of picric acid and bulk powders. The follow processes are same as the detonation exfoliation of MoS_2.

2.3. Characterizations

As-prepared MoS_2 as well as the WS_2 and h-BN samples were characterized by X-ray diffraction (XRD, Bruker, Germany), X-ray photoelectron spectroscopy (XPS, PHI-5400, Japan), high-resolution transmission electron microscopy (HR-TEM, Fischione M3000, USA) and atomic force microscopy (AFM, Bruker, Germany). The WS_2 and h-BN samples were also characterized by Raman spectroscopy (Jobin Yvon HR-800). XRD was performed using Cu target with the 2 theta scan range of 10–90°. XPS was performed using monochromatic aluminum KR X-rays. Thermo advantage software was used for XPS data analysis. The samples for HR-TEM and AFM examinations were dispersed in ethanol with ultrasonic treatment for 30 min before loading onto the carrier. Raman spectroscopy was performed using a HeNe laser with an excitation wavelength of 632.8 nm.

3. Results and discussion

3.1. Characterization of graphene-like MoS_2

To reveal the behavior and mechanism of detonation exfoliated in graphene-like MoS_2, different mixture mass ratios of picric acid and MoS_2 powder (1:2, 1:1, 2:1, 5:1, 10:1 and 20:1) were carried out in detonation exfoliating the bulk MoS_2. The 1:2 ratio detonated material shows little change of structure from the bulk MoS_2 due to the low detonation energy, so the results will not be discussed here. Phase analysis of bulk MoS_2, intercalation MoS_2 and intercalation-detonation MoS_2 materials exfoliated with different detonation mixture ratios were determined by X-ray diffraction (XRD), as shown in Fig. 1a,b. As seen in Fig. 1a, the main reflections of intercalation and 1:1 mixture ratio detonated MoS_2, such as (0 0 2), (1 0 0), (1 0 3) and (0 0 6), can be indexed to the 2H polytype of the MoS_2 crystal structure (JCPDS 37-1492). These results indicate that the intercalation and detonation procedures didn't change the hexagonal crystal structure of MoS_2.

A new molybdenum hemitrisulfide phase (Mo_2S_3, JCPD#65-6963) is present in the XRD patterns of intercalation-detonation MoS_2 samples detonated with mixture ratios of 2:1, 5:1, 10:1 and 20:1, as depicted in Fig. 1b. The main reflections are indexed to both 2H-MoS_2 and Mo_2S_3 crystals, indicating MoS_2 phase transformation by detonation, yet this almost did not appear for the 1:1 mixture ratio of detonated MoS_2.

Adiabatic method (Eq. (1)) [31] was used to calculate the mass fraction of MoS_2 and Mo_2S_3 in obtained products using the XRD data. Results show that the mass fraction of MoS_2 decreases with higher detonation mixture ratio, while the mass fraction of Mo_2S_3 increases, as seen in Table 1. Phase transition basically did not occur in the 1:1 detonated MoS_2 mixture ratio, which has 97.9% mass fraction of MoS_2 crystals. However, 20:1 detonated MoS_2 mixture ratio has only 12.9% mass fraction of MoS_2 crystals, and up to 87.1% mass fraction of Mo_2S_3 crystals. These results also indicate that the high detonation mixture ratio promotes the phase transform of the MoS_2 crystals, which was not expected.

$$W_X = \frac{I_X}{K_A^X \sum_{i=A}^{N} \frac{I_i}{K_A^i}} \quad (1)$$

Here, *W* is the mass fraction, X is the phase to be calculated, *K* is the reference intensity ratio, *I* is the actual intensity ratio, *i* is the phase order, and *A* is the internal standard phase, which is the MoS_2 phase here.

XPS measurements were carried out to characterize the chemical nature of bulk, intercalation and intercalation-detonation MoS_2 samples, as seen in Fig. 1c, d, e and f. The high resolution Mo 3d and S 2p spectra show that the peak locations of bulk, intercalation and 1:1 mixture ratio intercalation-detonation MoS_2 samples correspond to the Mo $3d_{3/2}$, Mo $3d_{5/2}$, S $2p_{1/2}$ and S $2p_{3/2}$ components of MoS_2 [32]. The Mo $3d_{5/2}$ binding energy peak located around 229.1 eV can be attributed to Mo^{4+} and the S $2p_{3/2}$ peak at 161–161.9 eV can be attributed to sulfides in Fig. 1c, e and Table 1. Corresponding Mo^{4+} of the Mo $3d_{5/2}$ peak can still be found in intercalation-detonation MoS_2 detonated with mixture ratios of 2:1, 5:1, 10:1 and 20:1 in Fig. 1d. However, a new binding energy peak appears at higher detonation mixture ratio. As seen in Fig. 1d, f, the new peak located at 228.1–228.6 eV can be indexed to Mo^{3+} [33], while the S $2p_{3/2}$ peak at 161.8–162.4 eV can be

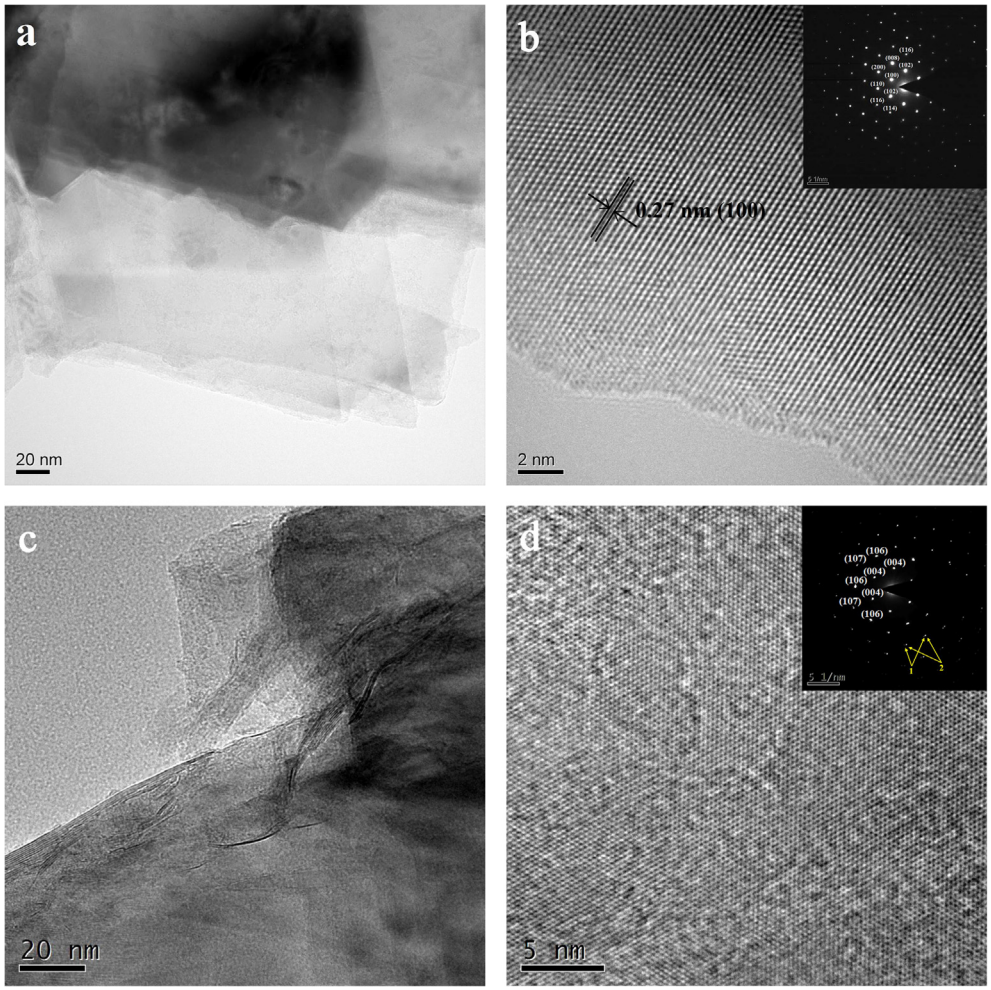

Fig. 2. TEM morphology of intercalation-detonation MoS_2 detonated with 1:1 (a, b) and 2:1 (c, d) mixture ratio.

indexed to the sulfides. Compared with the XRD analysis results, it can be confirmed that the new Mo_2S_3 phase was produced at high detonation mixture ratios, based on the XPS spectra.

At% ratio data of S and Mo was obtained from the XPS results, listed in Table 1. The data show that the S and Mo atomic ratios of bulk and 1:1 mixture ratio detonated MoS_2 samples are both 2, corresponding to the atomic ratio of the MoS_2 crystals. With the raise of detonation mixture ratio, the S and Mo atomic ratio decreases, while the 2:1 and 5:1 detonated mixture ratio samples have similar atomic ratio of about 1.6 and the atomic ratio of 20:1 detonated mixture ratio MoS_2 decreases to 0.729. The reduction of Mo atomic content also indicates MoS_2 decomposition at high detonation mixture ratio.

Fig. 2 and Fig. S1 (from Supporting Information) shows the TEM morphology of the intercalation-detonation MoS_2 samples detonated with 1:1, 2:1, 5:1, 10:1 and 20:1 mixture ratio. Layered structure can be seen at the edge of the 1:1 detonated mixture ratio sample in Fig. 2a, exhibiting multi-layer structure of the graphene-like MoS_2 nanosheet. High resolution TEM morphology in Fig. 2b shows high crystallinity of layered MoS_2 with 6.2 Å interplanar spacing. Selected area electron diffraction (SAED) pattern is shown in the inset of Fig. 2b and is well-indexed as pure hexagonal MoS_2 monocrystalline phase. Large area of folding thin sheet appears for the 2:1 detonated mixture ratio sample in Fig. 2c, exhibiting better layered structure. Besides, high resolution TEM morphology and the inset SAED pattern show the overlapped Moire fringes and two sets of diffraction spots (1 and 2 in the inset of Fig. 2d) with a small angle in Fig. 2d, which indicate that two different crystal orientations of graphene-like MoS_2 layer overlap in the sheet.

Big block of sheets with multilayer edge can be seen for the 5:1 detonated mixture ratio sample in Fig. S1a, exhibiting bad exfoliation process results. Moreover, directional Moire fringes are almost not visible in high resolution TEM morphology, and the multiple spots overlap with large angle can be seen in the SAED pattern in Fig. S1b. What's worse, Fig. S1c and e show large area of sheets with small particles on the layers for samples detonated with mixture ratio of 10:1 and 20:1. The SAED exhibits amorphous state pattern with polycrystalline diffraction rings in the 10:1 mixture ratio detonated sample, while the 20:1 detonated mixture ratio sample only shows amorphous state pattern in Fig. S1d and f. These results also indicate the MoS_2 crystalline phase transformation at high detonation mixture ratios.

AFM images of intercalation-detonation MoS_2 samples detonated with 1:1 and 2:1 mixture ratio are shown in Fig. 3. A piece of nanosheet lays on the substrate with fuzzy edge in Fig. 3a. The 1.35 nm calculated average thickness indicates the presence of 2 layers, where the thickness of MoS_2 sheets is 0.65 nm per layer, indicating that the layered structure of graphene-like MoS_2 was obtained. Pieces of nanosheets with thin edges can be seen in Fig. 3b and the average thickness is 0.7 nm, showing the single layer at the edge. These results indicate that the 2:1 detonation mixture ratio exhibits better exfoliation effect.

3.2. Detonation exfoliated mechanism of Graphene-like MoS_2

Based on the above analysis, the detonation mechanism of MoS_2 is proposed in the red frame of Fig. 4. Oxygen-containing functional groups intercalated MoS_2 was placed in a sealed stainless steel pressure vessel to be exfoliated by the explosion of picric acid. The high energy

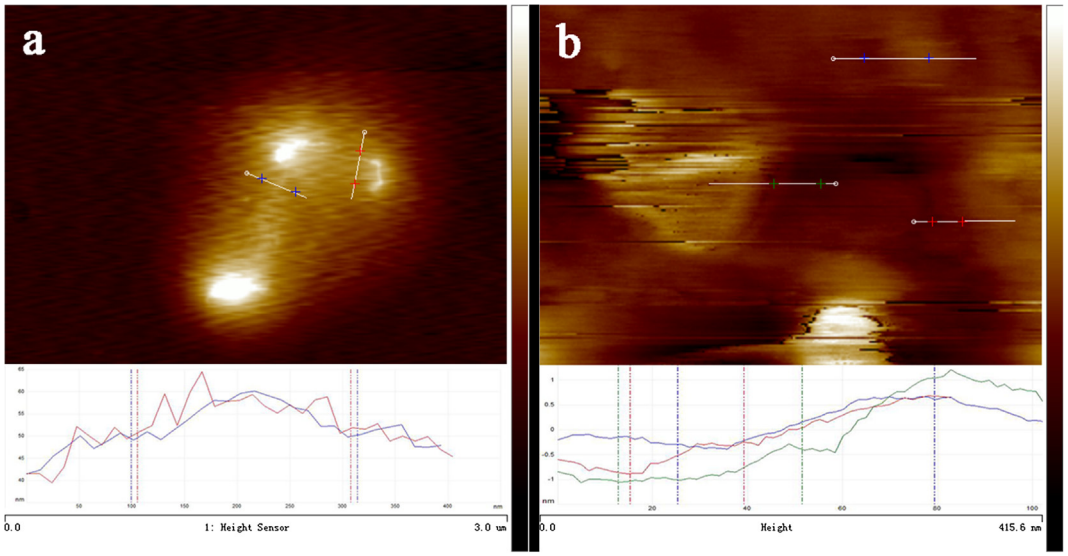

Fig. 3. AFM morphology of intercalation-detonation MoS_2 detonated with 1:1 (a) and 2:1 (b) mixture ratio.

detonation, on the one hand, causes cutting and separation of MoS_2 sheets by the high-speed shock wave. On the other hand, explosion of picric acid is a process of the decomposition reaction, which produces different kinds of gases, such as water vapor (H_2O), nitrogen (N_2) and carbon monoxide (CO), as shown in Eq. (2). The reaction between oxygen-containing groups (OH^+) and CO happened under high temperature, induced by the explosion, producing CO_2 and H_2O in Eq. (3). Expansion of the gases evolved into the interstices between the adjacent MoS_2 sheets also resulted in the MoS_2 exfoliation.

However, extreme high instantaneous temperature of about 2800 °C was produced as the high mixture ratio explosion happened (higher than 2:1), promoting part of MoS_2 decomposition to Mo_2S_3 and sulfur (Eq. (4)). Then sulfur reacts with the produced CO and water vapor to form hydrogen sulfide (H_2S) and carbon dioxide (CO_2), as shown in Eq. (5). Consequently, the final product is the exfoliated MoS_2 with part of decomposition result Mo_2S_3 after releasing gas by the high mixture ratio detonation.

$$2C_6H_3N_3O_7 = 3H_2O\uparrow + 3N_2\uparrow + 11CO\uparrow + C \quad (2)$$

$$[OH]^- + CO \rightarrow CO_2\uparrow + H_2O\uparrow \quad (3)$$

$$2MoS_2 = Mo_2S_3 + S \quad (4)$$

$$S + CO + H_2O = H_2S\uparrow + CO_2\uparrow \quad (5)$$

3.3. Detonation exfoliated of WS_2 and h-BN

Bulk WS_2 and h-BN were also exfoliated by detonation process using 1:1 mixture mass ratio of picric acid and raw powders. The follow processes are same as the detonation exfoliation of MoS_2. Fig. 5a shows the XRD patterns of the bulk and detonation exfoliated WS_2 material, along with the WS_2 standard peak. It can be seen from the figure that the main reflections of detonated WS_2, such as (0 0 2), (1 0 0) and (1 1 0), can be indexed to the WS_2 crystal structure (JCPDS 08-0237), indicating that the exfoliation process did not change the crystal structure of the hexagonal phase of the WS_2 material. The (0 0 2) peak is mainly derived from the scattering of WS_2 interlayer tungsten-tungsten atomic layer, which is reflected by the number and spacing of WS_2 layers stacked along the c-axis, while the (1 0 0) peak and (1 1 0) peak are intra-layer interactions. By further comparation, the weaker diffraction peaks (1 1 0), (2 0 0) and (2 1 1) of the elemental W can be found in the detonation exfoliated WS_2 material, indicating that a small

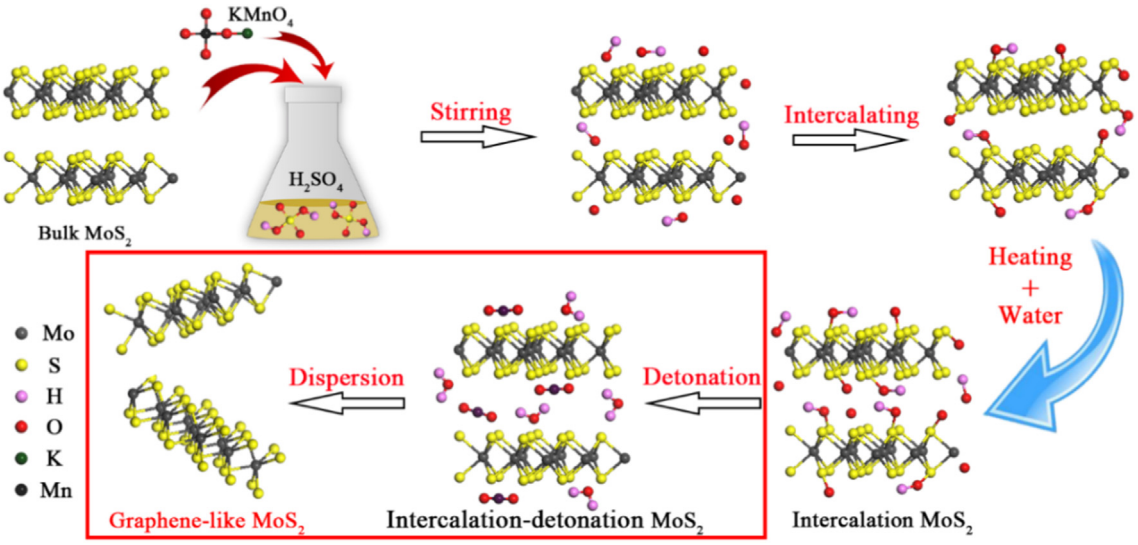

Fig. 4. Schematic illustration of the detonation exfoliated mechanism.

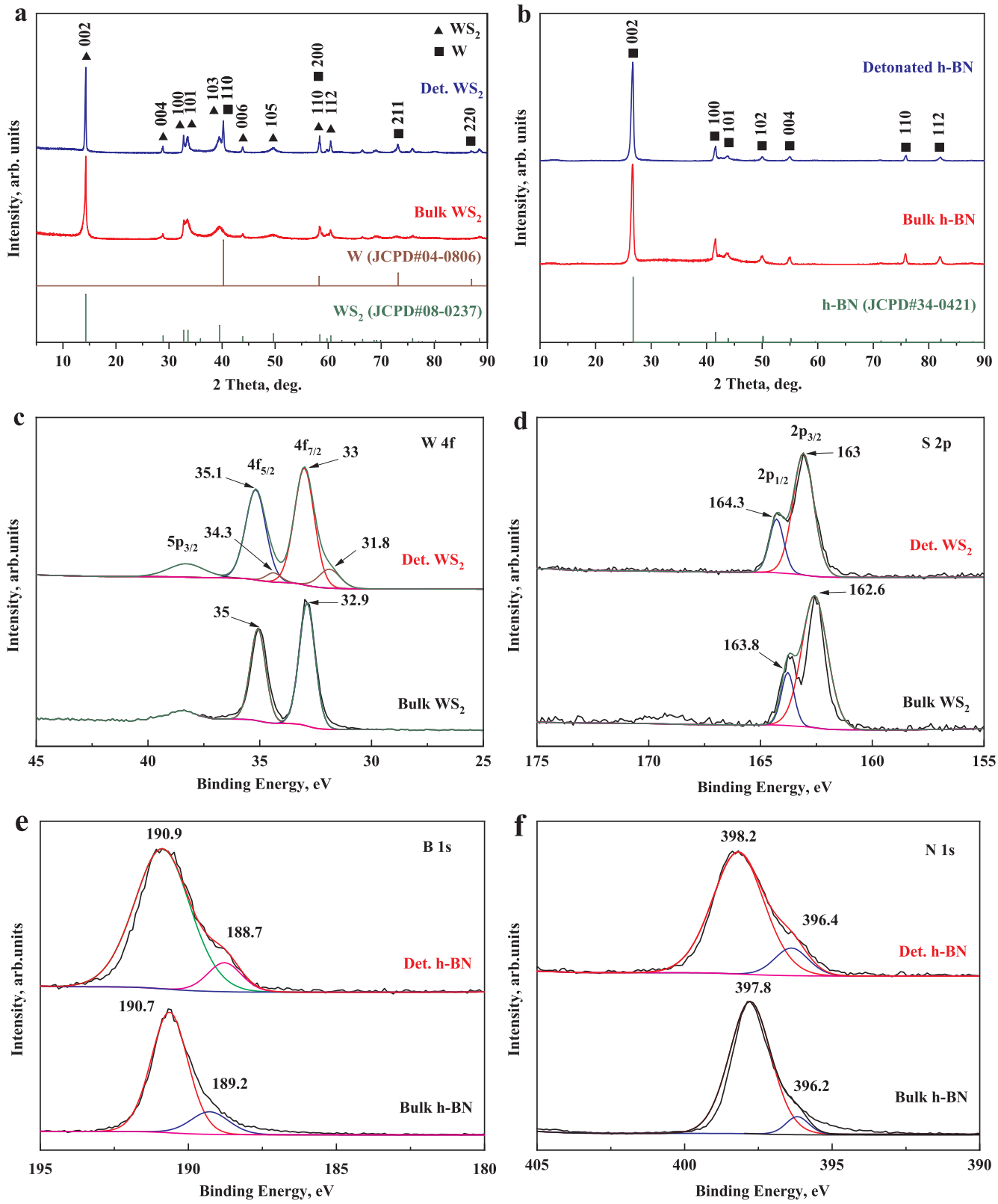

Fig. 5. XRD patterns and XPS spectra of bulk and detonation exfoliated WS_2 and h-BN: (a) XRD patterns of bulk and detonation exfoliated WS_2; (b) XRD patterns of bulk and detonation exfoliated h-BN; (c, d) XPS spectra of bulk and detonation exfoliated WS_2; (e, f) XPS spectra of bulk and detonation exfoliated h-BN.

amount of WS_2 decomposed during the explosion, and the elemental W was generated.

The XRD patterns of the bulk and detonation exfoliated h-BN materials in Fig. 5b shows the peak of (0 0 2), (1 0 0), (0 0 4), and (1 1 0), indexing to the h-BN crystal structure (JCPDS 34-0421). The XRD diffraction patterns indicate that the explosion reaction did not change the crystal structure of the hexagonal phase of the h-BN material.

High-resolution XPS W 4f and S 2p spectra of the bulk and

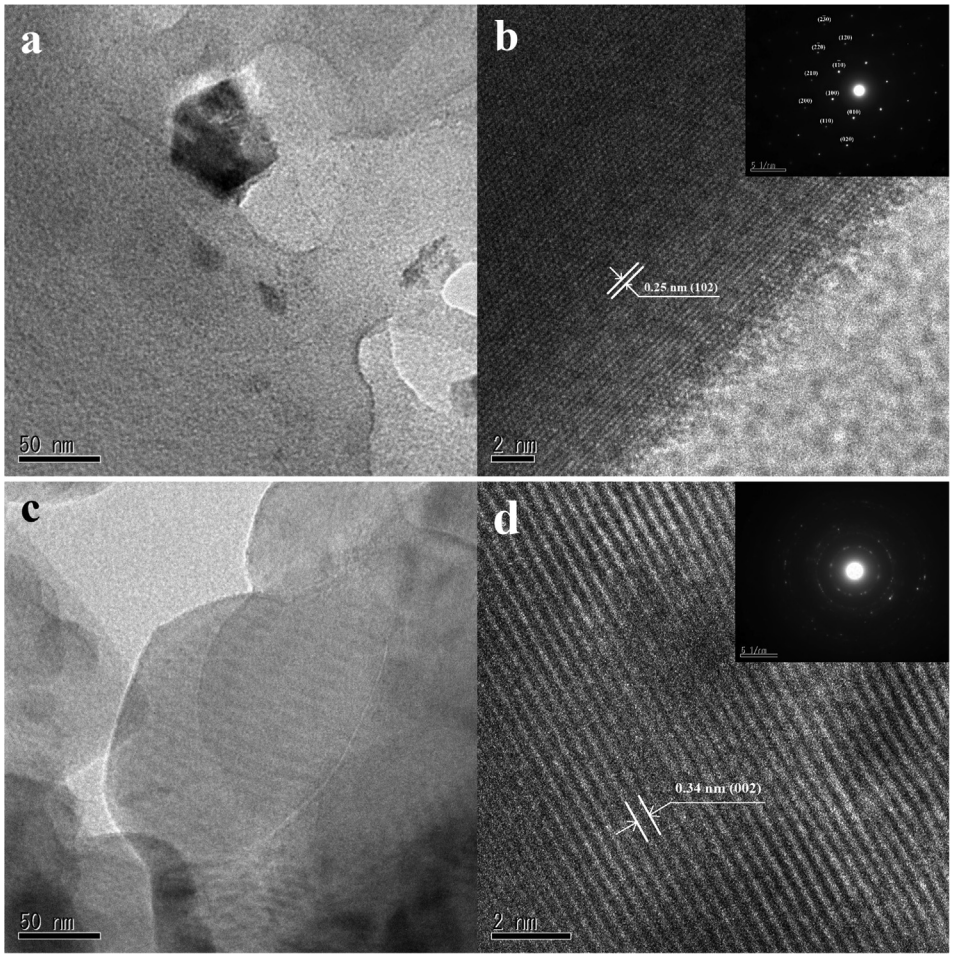

Fig. 6. TEM morphology of detonation exfoliated WS_2 (a, b) and h-BN (c, d) materials.

detonation exfoliated WS_2 materials can be seen in Fig. 5c, d. The figure shows that the peak locations of WS_2 materials correspond to the W $4f_{5/2}$, W $4f_{7/2}$, S $2p_{1/2}$ and S $2p_{3/2}$ components of WS_2. The W $4f_{7/2}$ binding energy peak located around 33 eV can be attributed to W^{4+} and the S $2p_{3/2}$ peak at 163 eV can be attributed to sulfides. A new binding energy peak at 31.8 eV appears in the W $4f_{7/2}$ peak of the detonation exfoliated WS_2 material, which corresponds to the simple substance of W as shown in Fig. 5c, but the peak intensity is small, indicating that the elemental W content is low. The results confirm that a small amount of new W elemental phase appeared after the WS_2 material exploded complex to the results of XRD patterns.

The high-resolution XPS spectra binding energy positions of the bulk h-BN B 1s and N 1s are at 190.7 eV and 397.8 eV, respectively (as seen in Fig. 5e and f). For detonation exfoliated h-BN, the binding energy positions of B 1s and N 1s spectra are at 190.9 eV and 398.2 eV, respectively, indicating that the h-BN material produced by high-energy detonation did not change the phase composition and atomic valence state.

TEM morphology of detonation exfoliated WS_2 and h-BN materials are show in Fig. 6. Fig. 6a shows the layered structure of the exfoliated WS_2 material. The high resolution TEM image in Fig. 6b clearly shows the high crystallinity layered WS_2 with a crystal plane spacing of 2.5 Å. Selected area electron diffraction (SAED) morphology shown in the insert of Fig. 6b shows the lattice diffraction spot of the hexagonal structure, which is well indexed as a pure WS_2 hexagonal single crystal phase. Fig. 6c shows the layered structure of the exfoliated h-BN material. The high resolution TEM image in Fig. 6d clearly shows the high crystallinity lamellar h-BN with a crystal plane spacing of 3.4 Å. The SAED morphology is shown in the insert of Fig. 6d, and the circular diffraction spot is well indexed as a polycrystalline multilayer h-BN hexagonal single crystal phase.

The AFM morphology of detonation exfoliated WS_2 and h-BN materials in Fig. S3 (from Supporting Information) showing that the average thickness of WS_2 is 0.742 nm and the thickness of h-BN can be found from 0.9 nm to 2.1 nm, which indicates that single layer of WS_2 material and few layers (less than 10 layers) h-BN were obtained, respectively. The Raman spectroscopy of bulk and detonation exfoliated WS_2 and h-BN also presents the high-crystallinity of materials (as seen in Supporting Information Fig. S3). All the results show that the high energy detonation preparation can strip out high-crystallinity single-layer WS_2 and few layers (less than 10 layers) h-BN nanosheets with good peeling effect.

4. Conclusion

In conclusion, the detonation exfoliated mechanism of graphene-like MoS_2 is systematically investigated by using the X-ray diffraction, X-ray photoelectron spectroscopy, high-resolution transmission electron and atomic force microscopy characterization methods. For comparison, 1:1, 2:1, 5:1, 10:1 and 20:1 mass ratio mixture of picric acid and MoS_2 powder were used to exfoliate the MoS_2 nanosheets by the detonation method. XRD, XPS and HR-TEM results show that pure hexagonal crystal structure of MoS_2 nanosheets was obtained with the 1:1 mass mixture ratio of the detonation procedure. 2:1 detonation mass mixture ratio produced monolayer MoS_2 nanosheets, but a MoS_2 spot can also be decomposed to Mo_2S_3 and S by high temperature of the explosion. With higher detonation mass mixture ratio, more MoS_2 is proposed to be decomposed, while only 12.9% of MoS_2 remained for

the 20:1 detonation mass mixture ratio. Therefore, the 1:1 detonation mass mixture ratio is the most suitable procedure to exfoliate graphene-like MoS_2 nanosheets. In addition, the success of detonation exfoliating bulk WS_2 and h-BN to single and few layers nanosheets shows the promising wide range of application of exfoliation in two-dimensional materials.

CRediT authorship contribution statement

Fan Yang: Investigation, Data curation, Writing - original draft. **Kuaishe Wang:** Supervision, Project administration. **Ping Hu:** Conceptualization, Methodology. **Xiaoyu Wang:** Investigation. **Tian Chang:** . **Zhenyu Chen:** . **Jie Deng:** . **Pengfa Feng:** Validation. **Alex A. Volinsky:** .

Declaration of Competing Interest

The authors declare that they have no known competing financial interests or personal relationships that could have appeared to influence the work reported in this paper.

Acknowledgements

This work was supported by the Youth Innovation Team of Shaanxi Universities (2019-2022), Outstanding Doctorate Dissertation Cultivation Fund of Xi'an University of Architecture and Technology (6040317013), Fok Ying Tung Education Foundation (171101), Youth Science and Technology New Star Project of Shaanxi Province Innovation Ability Support Plan (2017KJXX-63) and International scientific and technological cooperation program of Key Research and Development Program of Shaanxi Province (2018KW-053).

Appendix A. Supplementary material

Supplementary data to this article can be found online at https://doi.org/10.1016/j.apsusc.2020.145867.

References

[1] Q.H. Wang, K. Kalantar-Zadeh, A. Kis, J.N. Coleman, M.S. Strano, Electronics and optoelectronics of two-dimensional transition metal dichalcogenides, Nat. Nanotechnol. 7 (2012) 699–712.
[2] M.S. Xu, T. Liang, M.M. Shi, H.Z. Chen, Graphene-like two-dimensional materials, Chem. Rev. 113 (2013) 3766–3798.
[3] J.Y. Zheng, X.X. Yan, Z.X. Lu, H.L. Qiu, G.C. Xu, X. Zhou, P. Wang, X.Q. Pan, K.H. Liu, L.Y. Jiao, High-mobility multilayered MoS_2 flakes with low contact resistance grown by chemical vapor deposition, Adv. Mater. 29 (2017) 1604540.
[4] B. Radisavljevic, A. Radenovic, J. Brivio, V. Giacometti, A. Kis, Single-layer MoS_2 transistors, Nat. Nanotechnol. 6 (2011) 147–150.
[5] H. Li, Q. Zhang, C.C.R. Yap, B.K. Tay, T.H.T. Edwin, A. Olivier, D. Baillargeat, From bulk to monolayer MoS_2: evolution of raman scattering, Adv. Funct. Mater. 22 (2012) 1385–1390.
[6] X. Li, J.H. Li, X.H. Wang, J.X. Hu, X. Fang, X.Y. Chu, Z.P. Wei, J.J. Shan, X.C. Ding, Preparation, applications of two-dimensional graphene-like molybdenum disulfide, Integr. Ferroelectr. 158 (2014) 26–42.
[7] G.L. Frey, S. Elani, M. Homyonfer, Y. Feldman, R. Tenne, Optical-absorption spectra of inorganic fullerenelike MS_2 (M = Mo, W), Phys. Rev. B 57 (1998) 6666–6671.
[8] A. Splendiani, L. Sun, Y.B. Zhang, T. Li, J. Kim, C.-Y. Chim, G. Galli, F. Wang, Emerging photoluminescence in monolayer MoS_2, Nano Lett. 10 (2010) 1271–1275.
[9] D.Y. Chen, W.X. Chen, L. Ma, G. Ji, K. Chang, J.Y. Lee, Graphene-like layered metal dichalcogenide/graphene composites: synthesis and applications in energy storage and conversion, Mater. Today 17 (2014) 184–193.
[10] K. Dolui, I. Rungger, C.D. Pemmaraju, S. Sanvito, Possible doping strategies for MoS_2 monolayers: an ab initio study, Phys. Rev. B 88 (2013) 075420.
[11] K.F. Mak, C. Lee, J. Hone, J. Shan, T.F. Heinz, Atomically thin MoS_2: a new direct-gap semiconductor, Phys. Rev. Lett. 105 (2010) 136805.
[12] D. Sharma, A. Motayed, P.B. Shah, M. Amani, M. Georgieva, A. Glen Birdwell, M. Dubey, Q. Li, A.V. Davydov, Transfer characteristics and low-frequency noise in single- and multi-layer MoS_2 field-effect transistors, Appl. Phys. Lett. 107 (2015) 162102.
[13] D. MacMahon, A. Brothers, K. Florent, S. Kurinec, Layered structure of MoS_2 investigated using electron energy loss spectroscopy, Mater. Lett. 161 (2015) 96–99.
[14] V. Nicolosi, M. Chhowalla, M.G. Kanatzidis, M.S. Strano, J.N. Coleman, Liquid exfoliation of layered materials, Science 340 (2013) 1226419.
[15] J.N. Coleman, M. Lotya, A.O. Neill, S.D. Bergin, P.J. King, U. Khan, K. Young, A. Gaucher, S. De, R.J. Smith, I.V. Shvets, S.K. Arora, G. Stanton, H.-Y. Kim, K. Lee, G.T. Kim, G.S. Duesberg, T. Hallam, J.J. Boland, J.J. Wang, J.F. Donegan, J.C. Grunlan, G. Moriarty, A. Shmeliov, R.J. Nicholls, J.M. Perkins, E.M. Grieveson, K. Theuwissen, D.W. McComb, P.D. Nellist, V. Nicolosi, Two-dimensional nanosheets produced by liquid exfoliation of layered materials, Science 331 (2011) 568–571.
[16] X.Y. Yu, M.S. Prévot, K. Sivula, Multiflake thin film electronic devices of solution processed 2D MoS_2 enabled by sonopolymer assisted exfoliation and surface modification, Chem. Mater. 26 (2014) 5892–5899.
[17] G.J. Guan, S.Y. Zhang, S.H. Liu, Y.Q. Cai, M. Low, C.P. Teng, I.Y. Phang, Y. Cheng, K.L. Duei, B.M. Srinivasan, Y.G. Zheng, Y.W. Zhang, M.Y. Han, Protein induces layer-by-layer exfoliation of transition metal dichalcogenides, J. Am. Chem. Soc. 137 (2015) 6152–6155.
[18] K.R. Paton, E. Varrla, C. Backes, R.J. Smith, U. Khan, A.O. Neill, C. Boland, M. Lotya, O.M. Istrate, P. King, T. Higgins, S. Barwich, P. May, P. Puczkarski, I. Ahmed, M. Moebius, H. Pettersson, E. Long, J. Coelho, S.E.O. Brien, E.K. McGuire, B.M. Sanchez, G.S. Duesberg, N. McEvoy, T.J. Pennycook, C. Downing, A. Crossley, V. Nicolosi, J.N. Coleman, Scalable production of large quantities of defect-free few-layer graphene by shear exfoliation in liquids, Nat. Mater. 13 (2014) 624–630.
[19] E. Varrla, C. Backes, K.R. Paton, A. Harvey, Z. Gholamvand, J. McCauley, J.N. Coleman, Large-scale production of size-controlled MoS_2 nanosheets by shear exfoliation, Chem. Mater. 27 (2015) 1129–1139.
[20] M. Chen, H. Nam, H. Rokni, S.J. Wi, J.S. Yoon, P.Y. Chen, K. Kurabayashi, W. Lu, X.G. Liang, Nanoimprint-Assisted Shear Exfoliation (NASE) for producing multilayer MoS_2 structures as field-effect transistor channel arrays, ACS Nano 9 (2015) 8773–8785.
[21] K.C. Knirsch, N.C. Berner, H.C. Nerl, C.S. Cucinotta, Z. Gholamvand, N. McEvoy, Z.X. Wang, I. Abramovic, P. Vecera, M. Halik, S. Sanvito, G.S. Duesberg, V. Nicolosi, F. Hauke, A. Hirsch, J.N. Coleman, C. Backes, Basal-plane functionalization of chemically exfoliated molybdenum disulfide by diazonium salts, ACS Nano 9 (2015) 6018–6030.
[22] G. Eda, H. Yamaguchi, D. Voiry, T. Fujita, M.W. Chen, M. Chhowalla, Photoluminescence from chemically exfoliated MoS_2, Nano Lett. 11 (2011) 5111–5116.
[23] J. Zheng, H. Zhang, S.H. Dong, Y.P. Liu, C.T. Nai, H.S. Shin, H.Y. Jeong, B. Liu, K.P. Loh, High yield exfoliation of two-dimensional chalcogenides using sodium naphthalenide, Nat. Commun. 5 (2014) 2995.
[24] X.B. Fan, P.T. Xu, D.K. Zhou, Y.F. Sun, Y.C. Li, M.A.T. Nguyen, M. Terrones, T.E. Mallouk, Fast and efficient preparation of exfoliated 2H MoS_2 nanosheets by sonication-assisted lithium intercalation and infrared laser-induced 1T to 2H phase reversion, Nano Lett. 15 (2015) 5956–5960.
[25] N.R. Greiner, D.S. Phillips, J.D. Johnson, F. Volk, Diamonds in detonation soot, Nature 333 (1988) 440–442.
[26] H. Yin, P.W. Chen, C.X. Xu, X. Gao, Q. Zhou, Y. Zhao, L.T. Qu, Shock-wave synthesis of multilayer graphene and nitrogen-doped graphene materials from carbonate, Carbon 94 (2015) 928–935.
[27] X.H. Xie, X.J. Li, H.H. Yan, Detonation synthesis of zinc oxide nanometer powders, Mater. Lett. 60 (2006) 3149–3152.
[28] N. Luo, X.J. Li, K.X. Liu, L.M. Ye, T.W. Chen, Preparation of carbon-coated copper nanoparticles by detonation decomposition of copper ion doped sol-gel explosive precursors, J. Nanopart. Res. 15 (2013).
[29] F. Yang, P. Hu, K.S. Wang, Z.Y. Chen, B.L. Hu, R. Song, Q.W. Li, W.C. Cao, D.X. Liu, G. An, Z.Y. Jiang, Y.F. Li, A.A. Volinsky, Graphene-like MoS_2 prepared by a novel intercalation-detonation method, Mater. Lett. 188 (2017) 224–227.
[30] F. Yang, K.S. Wang, P. Hu, Z.Y. Chen, J. Deng, B.L. Hu, W.C. Cao, D.X. Liu, G. An, A.A. Volinsky, Oxidation layering mechanism of graphene-like MoS_2 prepared by the intercalation-detonation method, Nano Res. 11 (2018) 997–1003.
[31] F.H. Chung, Quantitative interpretation of X-ray diffraction patterns of mixtures. II. Adiabatic principle of X-ray diffraction analysis of mixtures, J. Appl. Crystallogr. 7 (1974) 526–531.
[32] P.P. Wang, H.Y. Sun, Y.J. Ji, W.H. Li, X. Wang, Three-dimensional assembly of single-layered MoS_2, Adv. Mater. 26 (2014) 964–969.
[33] X.W. Zhou, W. Zhao, J. Pan, Y.Q. Fang, F.Y. Wang, F.Q. Huang, Urchin-like Mo_2S_3 prepared via a molten salt assisted method for efficient hydrogen evolution, Chem. Commun. 54 (2018) 12714–12717.